Theories of Early Afterglow

P. Mészáros

Dept. of Astronomy & Astrophysics and Dept. of Physics, Pennsylvania State University, University Park, PA 16802, USA

Abstract. The rapid follow-up of gamma-ray burst (GRB) afterglows made possible by the multi-wavelength satellite *Swift*, launched in November 2004, has put under a microscope the GRB early post-burst behavior, This is leading to a significant reappraisal and expansion of the standard view of the GRB early afterglow behavior, and its connection to the prompt gamma-ray emission. In addition to opening up the previously poorly known behavior on minutes to hours timescales, two other new pieces in the GRB puzzle being filled in are the the discovery and follow-up of short GRB afterglows, and the opening up of the $z \gtrsim 6$ redshift range. We review some of the current theoretical interpretations of these new phenomena.

CHALLENGES POSED BY NEW SWIFT OBSERVATIONS

Compared to previous satellites, Swift has made a large difference on two main accounts. First, the sensitivity of the Burst Alert Detector (BAT, in the range 20-150 keV) is a factor ~ 5 higher than for the corresponding instruments in the predecessor CGRO-BATSE, BeppoSAX and HETE-2. Second, Swift can slew in less then 100 seconds in the direction determined by the BAT instrument, positioning its much higher angular resolution X-ray (XRT) and UV-Optical (UVOT) detectors on the burst [1]

As of December 2005, at an average rate of 2 bursts detected per week, over 100 bursts had been detected by BAT, of which 90% were followed promptly with the XRT within 350 s from the trigger, and about half within 100 s [2], while $\sim 30\%$ were detected with the UVOT [3]. Of these, over 23 resulted in redshift determinations. Ten short GRB were detected, of which five had detected X-ray afterglows, three had optical, and one had a radio afterglow, and five had a redshift determination.

The new observations brings the total redshift determinations to over 50 since 1997 when BeppoSAX enabled the first one. The redshifts based on Swift have a median $z \gtrsim 2$, which is a factor ~ 2 higher than the median of those previously culled via BeppoSAX and HETE-2, [5]. This can be ascribed to the higher sensitivity of BAT and the prompt accurate positions from XRT and UVOT, making possible ground-based detection at a stage when the afterglow is much brighter. The highest Swift-enabled redshift so far is in GRB 050904, obtained with Subaru, $z = 6.29$ [6], the second highest being GRB 050814 at $z = 5.3$, whereas the previous Beppo-SAX era record was $z = 4.5$. The relative paucity of UVOT detections versus XRT detections may be ascribed in part to this higher median redshift, and in part to the higher dust extinction at the implied shorter rest-frame wavelenghts for a given observed frequency [3], although additional effects may be at work too.

The BAT light curves show that in some of the bursts which fall in the

"long" category ($t_\gamma \gtrsim 2$ s) faint soft gamma-ray tails can be followed which extend the duration by a factor up to two beyond what BATSE could have detected [1]. A rich trove of information on the burst and afterglow physics has come from detailed XRT light curves, starting on average 100 seconds after the trigger, together with the corresponding BAT light curves and spectra. This suggests a canonical X-ray afterglow [18] with one or more of the following:
1) an initial steep decay $F_X \propto t^{-\alpha_1}$ with a temporal index $3 \lesssim \alpha_1 \lesssim 5$, and an energy spectrum $F_\nu \propto \nu^{-\beta_1}$ with energy spectral index $1 \lesssim \beta_1 \lesssim 2$ (or photon number index $2 \lesssim \Gamma = \alpha + 1 \lesssim 3$), extending up to a time $300\mathrm{s} \lesssim t_1 \lesssim 500\mathrm{s}$;
2) a flatter decay $F_X \propto t^{-\alpha_2}$ with $0.2 \lesssim \alpha_2 \lesssim 0.8$ and energy index $0.7 \lesssim \beta_2 \lesssim 1.2$, at times $10^3\mathrm{s} \lesssim t_2 \lesssim 10^4\mathrm{s}$;
3) a "normal" decay $F_X \propto t^{-\alpha_3}$ with $1.1 \lesssim \alpha_3 \lesssim 1.7$ and $0.7 \lesssim \beta_2 \lesssim 1.2$ (generally unchanged the previous stage), up to a time $t_3 \sim 10^5\mathrm{s}$, or in some cases longer;
4) In some cases, a steeper decay $F_X \propto t^{-\alpha_4}$ with $2 \lesssim \alpha_4 \lesssim 3$, after $t_4 \sim 10^5\mathrm{s}$;
5) In about half the afterglows, one or more X-ray flares are observed, sometimes starting as early as 100 s after trigger, and sometimes as late as 10^5s. The energy in these flares ranges from a percent up to a value comparable to the prompt emission (in GRB 050502b). The rise and decay times of these flares is unusually steep, depending on the reference time t_0, behaving as $(t - t_0)^{\pm \alpha_{fl}}$ with $3 \lesssim \alpha_{fl} \lesssim 6$, and energy indices which can be also steeper than during the smooth decay portions. The flux level after the flare usually decays to the value extrapolated from the value before the flare rise.

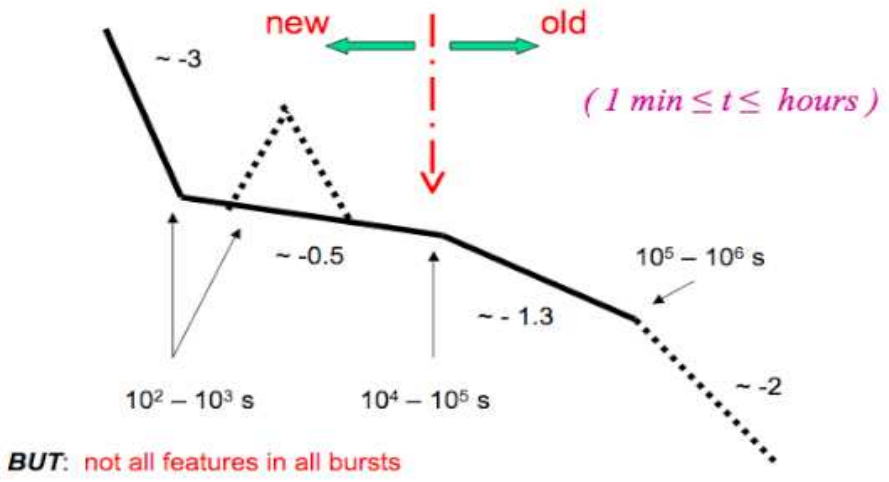

FIGURE 1. Schematic features seen by the XRT in bursts detected by Swift [16] (see text).

Another major advance achieved by Swift was the detection of the long burst GRB 050904, which broke through the astrophysically and psychologically important redshift barrier of $z \sim 6$. This burst was very bright, both in its prompt γ-ray emission ($E_{\gamma,iso} \sim 10^{54}$ erg) and in its X-ray afterglow. Prompt ground-based optical/IR upper limits and a J-band detection suggested a photometric redshift $z > 6$ [4]. Spectroscopic confirmation with the 8.2 m Subaru telescope gave a $z = 6.29$ [6]. There are several striking features to this burst. One is the enormous X-ray brightness, exceeding for a full day the X-ray brightness of the most distant X-ray quasar know to-date, SDSS J0130+0524, by up to

a factor 10^5 in the first minutes [7]. The implications as a tool for probing the IGM are thought-provoking. Another feature is the extremely variable X-ray light curve, showing many large amplitude flares extending up to at least a day. A third exciting feature is the report of a brief, very bright IR flash [8], comparable in brightness to the famous $m_V \sim 9$ optical flash in GRB 990123.

The third major advance from Swift was the discovery and localization of short GRB afterglows. As of December 2005 nine short bursts had been localized by Swift, while in the same period HETE-2 discovered two, and one was identified with the IPN network. In five of the Swift short bursts an X-ray afterglow was measured and followed up, with GRB 050709, 050724 and 051221a showing an optical afterglow, and 050724 also a radio afterglow, while 040924 had an optical afterglow but not an X-ray one [46]. These are the first afterglows detected for short bursts. Also, for the first time, host galaxies were identified for these short bursts, which in four cases are early type (ellipticals) and in two cases are irregular galaxies. The redshifts of four of them are in the range $z \sim 0.15 - 0.5$, while another one was initially given as $z = 0.8$ but more recently has been reported as $z \simeq 1.8$ [49]. The median z is $\lesssim 1/3 - 1/2$ that of the long bursts. There is no evidence for significant star formation in any of these host environments, which corresponds to what one would expect for neutron star mergers or neutron star-black hole mergers, the most often discussed progenitor candidates (it would also be compatible with other progenitors involving old compact stars).

The first short burst seen by Swift, GRB 05059b, was a low luminosity ($E_{iso} \sim 2 \times 10^{48}$ erg) burst with a simple power-law X-ray afterglow which could only be followed for $\sim 10^4$ s [36]. The third one, GRB 050724, was brighter, $E_{iso} \sim 3 \times 10^{50}$ erg, and could be followed in X-rays for at least 10^5 s [37]. The remarkable thing about this burst's X-ray afterglow is that it resembles the typical X-ray light curves described above for long GRB – except for the lack of a slow-decay phase, and for the short prompt emission which places it the the category of short bursts, as well as the elliptical host galaxy candidate. It also has X-ray flares, at 100 s and another one at 3×10^4 s. The first flare has the same fluence as the prompt emission, while the late flare has $\sim 10\%$ of that. The interpretation of these pose interesting challenges, as discussed below.

MODELS OF EARLY AFTERGLOWS IN LIGHT OF SWIFT

The afterglow is expected to become important after a time

$$t_{ag} = \mathrm{Max}[(3/4)(r_{dec}/2c\Gamma^2)(1+z)\ ,\ T] = \mathrm{Max}[10^2 (E_{52}/n_0)^{1/3} \Gamma_2^{-8/3} (1+z)|\mathrm{s}\ ,\ T]\ , \quad (1)$$

where the deceleration time is $t_{dec} \sim (3/4)(r_{dec}/2c\Gamma^2)$ and T is the duration of the prompt outflow, t_{ag} marking the beginning of the self-similar blast wave regime.

Denoting the frequency and time dependence of the afterglow spectral energy flux as $F_\nu(t) \propto \nu^{-\beta} t^{-\alpha}$, the late X-ray afterglow phases (3) and (4) described above are similar to those known previously from Beppo-SAX. (For a review of this earlier behavior and its modeling see e.g. [9]). The "normal" decay phase (3), with temporal decay indices $\alpha \sim 1.1 - 1.5$ and spectral energy indices $\beta \sim 0.7 - 1.0$, is what is expected from the

evolution of the forward shock in the Blandford-McKee self-similar late time regime, under the assumption of synchrotron emission.

The late steep decay decay phase (4) of §, occasionally seen in Swift bursts, is naturally explained as a jet break, when the decrease of the ejecta Lorentz factor leads to the light-cone angle becoming larger than the jet angular extent, $\Gamma_j(t) \gtrsim 1/\theta_j$ (e.g. [9]). It is noteworthy, however, that this final steepening has been seen in less than $\sim 10\%$ of the Swift afterglows, and then with reasonable confidence mainly in X-rays. The corresponding optical light curve breaks have been few, and not well constrained. This is unlike the case with the ~ 20 Beppo-SAX bursts, for which an achromatic break was reported in the optical [10], while in some of the rare cases where an X-ray or radio break was reported it occurred at a different time [11]. The relative paucity of optical breaks in Swift afterglows may be an observational selection effect due to the larger median redshift, and hence fainter and redder optical afterglow at the same observer epoch, as well as perhaps reluctance to commit large telescope time on more frequently reported bursts (an average, roughly, of 2/month with Beppo-SAX versus 2/week with Swift).

Steep decay

Among the new early afterglow features detected by Swift, the steep initial decay phase $F_\nu \propto t^{-3} - t^{-5}$ in X-rays of the long GRB afterglows is one of the most puzzling. There could be several possible reasons for this. The most immediate of these would be the cooling following cessation of the prompt emission (internal shocks or dissipation). If the comoving magnetic field in the emission region is random [or transverse], the flux per unit frequency along the line of sight in a given energy band, as a function of the electron energy index p, decays as $F_\nu \propto t^{-\alpha}$ with $\alpha = -2p\ [(1-3p)/2]$ in the slow cooling regime, where $\beta = (p-1)/2$, and it decays as $\alpha = -2(1+p),\ [-(2-3p)/2]$ in the fast cooling regime where $\beta = p/2$, i.e. for the standard $p = 2.5$ this would be $\alpha = -5,\ [-3.25]$ in the slow cooling or $\alpha = -7,\ [-2.75]$ in the fast cooling regime, for random [transverse] fields [12]. In some bursts this may be the explanation, but in others the time and spectral indices do not correspond well.

Currently the most widely considered explanation for the fast decay, either in the initial phase (1) or in the steep flares, attributes it to the off-axis emission from regions at $\theta > \Gamma^{-1}$ (the curvature effect, or high latitude emission [13]. In this case, after the line of sight gamma-rays have ceased, the off-axis emission observed from $\theta > \Gamma^{-1}$ is $(\Gamma\theta)^{-6}$ smaller than that from the line of sight. Integrating over the equal arrival time region, this flux ratio becomes $\propto (\Gamma\theta)^{-4}$. Since the emission from θ arrives $(\Gamma\theta)^2$ later than from $\theta = 0$, the observer sees the flux falling as $F_\nu \propto t^{-2}$, if the flux were frequency independent. For a source-frame flux $\propto \nu'^{-\beta}$, the observed flux per unit frequency varies then as

$$F_\nu \propto (t - t_0)^{-2-\beta} \tag{2}$$

i.e. $\alpha = 2 + \beta$. This "high latitude" radiation, which for observers outside the line cone at $\theta > \Gamma^{-1}$ would appear as prompt γ-ray emission from dissipation at radius r, appears to observers along the line of sight (inside the light cone) to arrive delayed by $t \sim r\theta^2/2c)$ relative to the trigger time, and its spectrum is softened by the Doppler factor $\propto t^{-1}$

into the X-ray observer band. For the initial prompt decay, the onset of the afterglow (e.g. phases 2 or 3), which also come from the line of sight, may overlap in time with the delayed high latitude emission. In equation (2) t_0 can be taken as the trigger time, or some value comparable or less than by equation (1). This can be used to constrain the prompt emission radius [26]. When $t_{dec} < T$, the emission can have an admixture of high latitude and afterglow, and since the afterglow has a steeper spectrum than the high latitude (which has a prompt spectrum), one can have steeper decays [24]. Values of t_0 closer to the onset of the decay also lead to steeper slopes. Structured jets, when viewed on-beam produce essentially the same slopes as homogeneous jets, while off-beam observing can lead to shallower slopes [14]. For the flares, if their origin is assumed to be internal (e.g. some form of late internal shock or dissipation) the value of t_0 is just before the flare, e.g the observer time at which the internal dissipation starts to be observable [17]. This interpretation appears, so far, compatible with most of the Swift afterglows [16, 18, 19].

Alternatively, the initial fast decay could be due to the emission of a cocoon of exhaust gas [20], where the temporal and spectral index are explained through an approximately power-law behavior of escape times and spectral modification of multiply scattered photons. The fast decay may also be due to the reverse shock emission, if inverse Compton up-scatters primarily synchrotron optical photons into the X-ray range. The decay starts after the reverse shock has crossed the ejecta and electrons are no longer accelerated, and may have both a line of sight and an off-axis component [21]. This poses strong constraints on the Compton-y parameter, and cannot explain decays much steeper than $\alpha = -2$, or $-2-\beta$ if the off-axis contribution dominates. Models involving bullets, whose origin, acceleration and survivability is unexplained, could give a prompt decay index $\alpha = -3-5$ [15], but imply a bremsstrahlung energy index $\beta \sim 0$ which is not observed in the fast decay, and require fine-tuning. Finally, a patchy shell model, where the Lorentz factor is highly variable in angle, would produce emission with $\alpha \sim -2.5$. Thus, such mechanisms may explain the more gradual decays, but not the more extreme $\alpha = -5, -7$ values encountered in some cases.

Shallow decay

The slow decay portion of the X-ray light curves ($\alpha \sim -0.3-0.7$), ubiquitously detected by Swift, is not entirely new, having been detected in a few cases by BeppoSAX. This, as well as the appearance of wiggles and flares in the X-ray light curves after several hours were the motivation for the “refreshed shock" scenario [22, 23]. Refreshed shocks can flatten the afterglow light curve for hours or days, even if the ejecta is all emitted promptly at $t = T \lesssim t_\gamma$, but with a range of Lorentz factors, say $M(\Gamma) \propto \Gamma^{-s}$, where the lower Γ shells arrive much later to the foremost fast shells which have already been decelerated. Thus, for an external medium of density $\rho \propto r^{-g}$ and a prompt injection where the Lorentz factor spread relative to ejecta mass and energy is $M(\Gamma) \propto \Gamma^{-s}$, $E(\Gamma) \propto \Gamma^{-s+1}$, the forward shock flux temporal decay is given by [23]

$$\alpha = [(g-4)(1+s) + \beta(24-7g+sg)]/[2(7+s-2g)] \, . \tag{3}$$

It needs to be emphasized that in this model all the ejection can be prompt (e.g. over the duration $\sim T$ of the gamma ray emission) but the low Γ portions arrive at (and refresh) the forward shock at late times, which can range from hours to days. I.e., it is not the central engine which is active late, but its effects are seen late. Fits of such refreshed shocks to observed shallow decay phases in Swift bursts [28] lead to a Γ distribution which is a broken power law, extending above and below a peak around ~ 45.

Another version of refreshed shocks, on the other hand, does envisage central engine activity extending for long periods of time, e.g. $\lesssim$ day (in contrast to the $\lesssim$ minutes engine activity in the model above). Such long-lived activity may be due to continued fall-back into the central black hole [32] or a magnetar wind [27]. One characteristic of both types of refreshed models is that after the refreshed shocks stop and the usual decay resumes, the flux level shows a step-up relative to the previous level, since new energy has been injected.

From current analyses, the refreshed shock model is generally able to explain the flatter temporal X-ray slopes seen by Swift, both when it is seen to join smoothly on the prompt emission (i.e. without an initial steep decay phase) or when seen after an initial steep decay. Questions remain concerning the interpretation of the fluence ratio in the shallow X-ray afterglow and the prompt gamma-ray emission, which can reach $\lesssim 1$ [24]. This requires a higher radiative efficiency in the prompt gamma-ray emission than in the X-ray afterglow. One might speculate that this might be achieved if the prompt outflow is Poynting-dominated. Alternatively, a more efficient afterglow might emit more of its energy in other bands, e.g. in GeV, or IR. Or [30] a previous mass ejection might have emptied a cavity into which the ejecta moves, leading to greater efficiency at later times, or otherwise the energy fraction going into the electrons increases $\propto t^{1/2}$.

X-ray flares

Refreshed shocks can also explain some of the X-ray flares whose rise and decay slopes are not too steep. However, this model encounters difficulties with the very steep flares with rise or decay indices $\alpha \sim \pm 5 - 7$, such as inferred from the giant flare of GRB 0500502b [29] around 300 s after the trigger. Also, the flux level increase in this flare is a factor ~ 500 above the smooth afterglow before and after it, implying a comparable energy excess in the low versus high Γ material. An explanation based on inverse Compton scattering in the reverse shock [21] can explain a single flare at the beginning of the afterglow, with not too steep decay. For multiple flares, models invoking encountering a lumpy external medium have generic difficulties explaining steep rises and decays [16], although extremely dense, sharp-edged lumps, if they exist, might satisfy the steepness [31].

Currently the more widely considered model for the flares ascribes them to late central engine activity [16, 18, 19]. The strongest argument in favor of this is that the energy budget is more easily satisfied, and the fast rise/decay is straightforward to explain. In such a model the flare energy can be comparable to the prompt emission, the fast rise comes naturally from the short time variability leading to internal shocks (or to rapid reconnection), while the rapid decay may be due to the high latitude emission following

the flare, with t_0 reset to the beginning of each flare (see further discussion in [17]). However, some flares are well modeled by refreshed forward shocks, while in others this is clearly ruled out and a central engine origin is better suited [41]. Aside from the phenomenological desirability based on energetics and timescales, a central engine origin is conceivable, within certain time ranges, based on numerical models of the core collapse origin in long bursts. These are interpreted as being due to core collapse of a massive stellar progenitor, where continued infall into fast rotating cores can continue for a long time [32]. However, large flares with a fluence which is a sizable fraction of the prompt emission occurring hours later remain difficult to understand. It has been argued that gravitational instabilities in the infalling debris torus can lead to lumpy accretion [33]. Alternatively, if the accreting debris torus is dominated by MHD effects, magnetic instabilities can lead to extended, highly time variable accretion [34].

Short burst afterglows

Swift, and in smaller numbers HETE-2, have provided the first bona fide short burst X-ray afterglows followed up starting ~ 100 s after the trigger, leading to localizations and redshifts. In the first of these, GRB 050509b [36] the extrapolation of the prompt BAT emission into the X-ray range, and the XRT light curve from 100 s to about 1000 s (after which only upper limits exist, even with Chandra, due to the faintness of the burst) can be fitted with a single power law of $\alpha \sim 1.2$, or separately as $\alpha_{BAT} = -1.3$ and $\alpha_{XRT} = 1.1$. The X-ray coverage was sparse due to orbital constraints, the number of X-ray photons being small, and no optical transient was identified, probably due to the faintness of the source. An optical host was however identified [39], an irregular galaxy at $z = 0.16$ (and the observations ruled out any supernova association). On the other hand, GRB 050724 was relatively bright, and besides X-rays, it also yielded both a decaying optical and a radio afterglow [40]. This burst, together with the greater part of other short bursts, is associated with an elliptical host galaxy. It also had a low-luminosity soft gamma-ray extension of the short hard gamma-ray component (which would have been missed by BATSE), and it had an interesting X-ray afterglow extending beyond 10^5 s [37]. The soft gamma-ray extension, lasting up to 200 s, when extrapolated to the X-ray range overlaps well with the beginning of the XRT afterglow, which between 100 and 300 s has $\alpha \sim -2$, followed by a much steeper drop $\alpha \sim -5 - 7$ out to $\sim 600s$, then a more moderate decay $\alpha \sim -1$. An unexpected feature is a strong flare peaking at 5×10^4 s, whose energy is 10% of the prompt emission, while its amplitude is a 10 times increase over the preceding slow decay. With about a half dozen of reasonably identified objects, the distribution of shorts bursts in redshift space and among host galaxy types, including fewer spiral/irregulars and more ellipticals, is typical of old population progenitors, such as neutron star binaries or black hole-neutron star binaries [38].

The main challenges posed by the short burst afterglows are the relatively long, soft tail of the prompt emission, and the strength and late occurrence of the flares. A possible explanation for the extended long soft tails ($\sim 100s$) may be that the compact binary progenitor is a black hole - neutron star system [37], for which analytical and numerical arguments ([44], and references therein) suggest that the disruption and swallowing by

the black hole may lead to a complex and more extended accretion rate than for double neutron stars. The flares, for which the simplest interpretation might be as refreshed shocks (which would be compatible with a short engine duration $T \lesssim t_\gamma \sim 2$ s, for a Lorentz factor distribution), requires the energy in the slow material to be at least ten times as energetic as the fast material responsible for the prompt emission, for the GRB 050724 flare at 10^4 s. The rise and decay times are moderate enough for this interpretation. Another interpretation might be an accretion-induced collapse of a white dwarf in a binary, leading to a flare when the fireball created by the collapse hits the companion [45], which might explain moderate energy one-time flares. However, for repeated, energetic flares, as also in the long bursts, the total energetics are easier to satisfy if one postulates late central engine activity (lasting at least half a day), containing $\sim 10\%$ of the prompt fluence [37]. A possible way to produce this might be temporary choking up of an MHD outflow [34] (c.f. [43]), which might also imply a linear polarization of the X-ray flare [42]. Such MHD effects could plausibly also explain the initial ~ 100 s soft tail. However, a justification for substantial $\gtrsim 10^5$ s features remains so far on tentative grounds.

The similarity of the X-ray afterglow light curve with those of long bursts is, in itself, an argument in favor of the prevalent view that the afterglows of both long and short bursts can be described by the same paradigm, independently of any difference in the progenitors. This impression is reinforced by the fact that the X-ray light curve temporal slope is, on average, that expected from the usual forward shock afterglow model, and that in two short bursts (so far) there is evidence for what appears to be a jet break [40, 35]. However, while similar to zeroth order, the first order differences are revealing: the average isotropic energy is factor ~ 100 smaller, while the average jet opening angle (based on two breaks) is a factor ~ 2 larger [46, 35]. Using the standard afterglow theory, the bulk Lorentz factor decay can be expressed through $\Gamma(t_d) = 6.5(n_o/E_{50})^{1/8} t_d^{-3/8}$, where $t_d = (t/\mathrm{day})$, n_o is the external density in units of cm^{-3}, and E_{50} is the isotropic equivalent energy in units of 10^{50} ergs. If the jet break occurs at $\Gamma(t_{br}) = \theta_j^{-1}$ the jet opening angle and the total jet energy E_j are

$$\theta_j = 9^o (n_o/E_{50})^{1/8} t_{d,br}^{3/8} \ , E_j = \pi \theta_j^2 E \sim 10^{49} n_o^{1/4} (E_{50} t_{d,br})^{3/4} \ \mathrm{erg} \ . \qquad (4)$$

For the first two well studied afterglows GRB 050709 and GRB 050724, together with the standard afterglow expressions for the flux level as a function of time before and after the break, this leads to fits [35] which are not completely determined, allowing for GRB050709 either a very low or a moderately low external density, and for GRB050724 a moderately low to large external density. The main uncertainty is in the jet break time, which is poorly sampled, and so far mainly in X-rays. As brighter short bursts are occasionally detected, e.g. GRB 051221A, the chances of tighter constraints on jet breaks should increase.

Prompt optical flashes and high redshift afterglows

Optical/UV afterglows have been detected with the Swift UVOT telescope in roughly half the bursts for which an X-ray afterglow was seen. For a more detailed discussion of

the UVOT afterglow observations see [3]. Of particular interest is the ongoing discussion on whether “dark GRB" are really optically deficient, or the result of observational bias [5]. Another puzzle is the report of a bimodal intrinsic brightness distribution in the rest-frame R-band [47, 48]. This suggests possibly the existence of two different classes of long bursts, or at least two different types of environments.

Compared to a few years ago, a much larger role is being played by ground-based robotic optical follow-ups, due to the increased rate of several arc-second X-ray alerts from XRT, and the larger number of robotic telescopes brought on-line in the last years. For the most part, these detections have yielded optical decays in the $\gtrsim$ few 100 s range, initial brightness $m_V \sim 14-17$ and temporal decay slopes $\alpha \sim 1.1-1.7$ previously associated with the evolution of a forward shock [46, 49], while in a few cases a prompt optical detection was achieved in the first 12-25 s.

The most exciting prompt robotic IR detection (and optical non-detection) is that of GRB 050904 [8, 4]. This object, at the unprecedented high redshift of $z = 6.29$ [6], has an X-ray brightness exceeding for a day that of the brightest X-ray quasars [7], and its O/IR brightness in the first 500 s (observer time) was comparable to that of the extremely bright ($m_V \sim 9$) optical flash in GRB 990123, with a similarly steep time-decay slope $\alpha \sim 3$ [8]. Such prompt, bright and steeply decaying optical emission is expected from the reverse shock as it crosses the ejecta, marking the start of the afterglow [50]. However, aside from the two glaring examples of 990123 and 05094, in the last six years there have been less than a score of other prompt optical flashes, typically with more modest initial brightnesses $m_v \gtrsim 13$. There are a number of possible reasons for this paucity of optically bright flashes, if ascribed to reverse shock emission. One is the absence or weakness of a reverse shock, e.g. if the ejecta is highly magnetized [50]. A moderately magnetized ejecta is in fact favored for some prompt flashes [51]. Alternatively, the deceleration might occur in the thick-shell regime ($T \gg t_{dec}$. see eq. (1), which can result in the reverse shock being relativistic, boosting the optical reverse shock spectrum into the UV [52]. Another possibility, for a high comoving luminosity, is copious pair formation in the ejecta, causing the reverse shock spectrum to peak in the IR [53]. Since both GRB 990123 and GRB 050904 had $E_{iso} \sim 10^{54}$ erg, among the top few percent of all bursts, the latter is a distinct possibility, compatible with the fact that the prompt flash in GRB 050904 was bright in the IR I-band but not in the optical. On the other hand, the redshift $z = 6.29$ of this burst, and a Ly-α cutoff at ~ 800 nm would also ensure this (and GRB 990123, at $z = 1.6$, was detected in the V-band). However, the observations in these two objects but a suppression in lower E_{iso} objects appears compatible with having a relativistic (thick shell) reverse shock with pair formation.

ACKNOWLEDGMENTS

I am grateful to the Swift team for collaborations and to NASA NAG5 13286 for support.

REFERENCES

1. Gehrels, N, 2005, these procs.
2. Burrows, D, 2005, these proceedings; also astro-ph/0511039
3. Roming, P, 2005, these proceedings; also astro-ph/050927
4. Haislip, J, et al, 2005, Nature, subm. (astro-ph/0509660)
5. Berger, E, et al, 2005, ApJ 634:501
6. Kawai, N. et al, 2005, astro-ph/0512052
7. Watson, D. et al, 2005, ApJ(Lett) in press (astro-ph/0509640)
8. Boër, M, et al, 2005, Nature, subm (astro-ph/0510381)
9. Zhang, B and Mészáros, P, 2004, Internat.J.Mod.Phys. A, 19:2385
10. Frail, D et al., ApJ 562:L155
11. Berger, E, Kulkarni, SR and Frail, D, 2003, ApJ 590:379
12. Mészáros, P and Rees, MJ, 1999, MNRAS, 306:L39
13. Kumar, P and Panaitescu, A, 2000, ApJ 541:L51
14. Dyks, J, Zhang, B, Fan, YZ, 2005, ApJ subm (astro-ph/0511699)
15. Dado, S, et al, astro-ph/0512196
16. Zhang, B. et al, 2006, ApJ in press (astro-ph/0508321)
17. Zhang, B. et al, these proceedings
18. Nousek, J, et al, ApJ, in press (astro-ph/0508332)
19. Panaitescu, A, et al, 2005, MNRAS in press (astro-ph/0508340)
20. Pe'er, A, Mészáros, P and Rees, MJ, 2006, in prep.
21. Kobayashi, S, et al, 2005, ApJ subm (astro-ph/0506157)
22. Rees, MJ and Mészáros, P, 1998, ApJ, 496:L1
23. Sari, R and Mészáros, P, 2000, ApJ, 535:L33
24. O'Brien, P. et al, in preparation
25. Dyks, J, Zhang, B and Fan, YS, ApJ subm (astro-ph/0511699)
26. Lazzati, D. and Begelman, M, astro-ph/0511658
27. Zhang, B and Mészáros, P, 2001, ApJ 552:L35
28. Granot, J and Kumar, P, ApJ subm (astro-ph/0511049)
29. Burrows, D, et al, 2005a, Science, 309, 1833
30. Ioka, K, et al, astro-ph/0511749
31. Dermer, C, 2005, these proceedings
32. Woosley, S, 2005, these proceedings
33. Perna, R, Armitage, and Zhang, B, ApJ in press (astro-ph/0511506)
34. Proga, D and Begelman, M, 2003, ApJ, 592:767
35. Panaitescu, A, 2005, ApJ subm (astro-ph/0511588)
36. Gehrels, N. et al, 2005, Nature, 437:851
37. Barthelmy, S., 2005, Nature, in press (astro-ph/0511579)
38. Nakar, E, Gal-Yam, A and Fox, D, (astro-ph/0511254)
39. Fox, D. et al, 2005, Nature, 437:845
40. Berger, E, et al, 2005, ApJ, 634:501
41. Wu, X.F. et al, ApJ subm (astro-ph/0512555)
42. Fan, YZ, Proga, D and Zhang, B, 2005, astro-ph/0509019
43. Van Putten, M and Ostriker, A, 2001, ApJ 552:L31
44. Davies, M, Levan, A, King, A, 2005, MNRAS 365:54
45. MacFadyen, A, 2005, these proceedings
46. Fox, D, 2005, these proceedings.
47. Liang, EW and Zhang, B, 2005, astro-ph/0508510
48. Nardini, M, et al, D, 2005, astro-ph/0508447
49. Berger, E, 2005, these proceedings
50. Mészáros, P and Rees, MJ, 1997, ApJ 476:232
51. B. Zhang, S. Kobayashi and P. Mészáros, 2003, ApJ, 589:861
52. Kobayashi, S, 2000, ApJ, 545:807
53. Mészáros, P, Ramirez-Ruiz, E, Rees, MJ, Zhang, B, 2002, ApJ, 578:812